CROSS SECTIONS, RECOIL RANGES, AND ANGULAR DISTRIBUTIONS OF NUCLEI PRODUCED IN 20-200 MEV ALPHA BOMBARDMENT OF ^{59}Co

T. Mroz, P.P. Singh, M. Fatyga, H.J. Karwowski, and S.E. Vigdor
Indiana University Cyclotron Facility, Bloomington, Indiana 47405

J. Jastrzebski
Institute of Nuclear Research, Swierk, Poland

Using the in-beam γ-ray and off-beam activation techniques[1] we have measured production cross sections for various residual nuclei and integral recoil ranges of radioactive nuclei formed in the 20-200 MeV alpha particle bombardment of ^{59}Co targets. We also measured angular distributions of radioactive recoils at 80 and 118 MeV bombarding energy.

The in-beam γ-ray measurements were performed using Ge(Li) detectors with a resolution of ~2.5 keV at 1330 keV γ-energy. Cross sections for the production of individual final nuclei were obtained by summing observed cross sections for γ-rays corresponding to transition to the ground state and to the known isomeric states of the respective nucleus.[1]

The recoil ranges were measured by bombarding a stack of ^{59}Co targets sandwiched between kapton or Al catchers and interspersed by aluminum energy-degrading foils. The ratio of the activity measured in a catcher to the total activity in the catcher plus the preceding target foil yields a good measure of the projection of

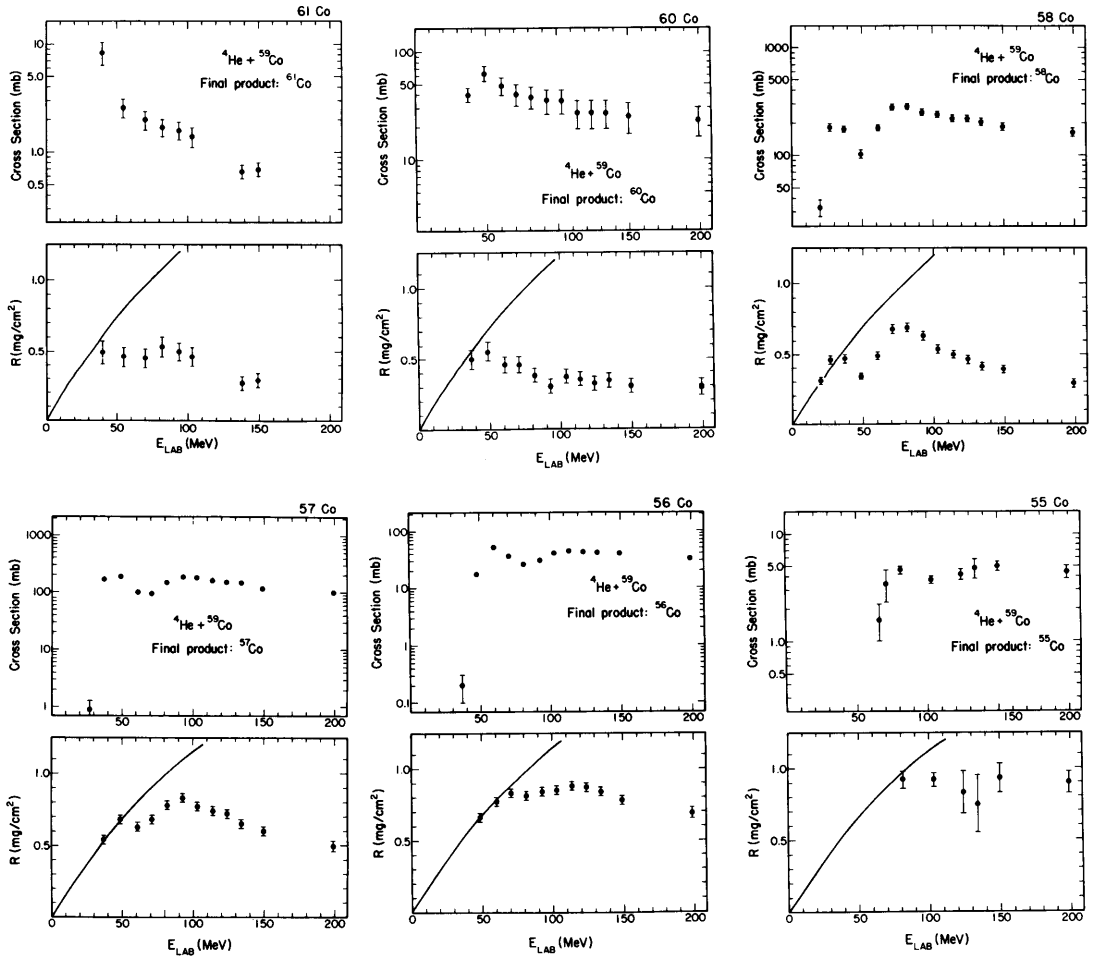

Figure 1. Cross sections (σ) and integral recoil ranges (R) plotted as a function of bombarding α-energy for the radioactive products of ^{4}He+^{59}Co reaction. The solid lines in the recoil ranges part of the figure are calculated assuming a full momentum transfer to the compound nucleus.

the recoil range on the beam axis.

The angular distributions of the radioactive products were measured by bombarding thin (150-200 $\mu g/cm^2$) ^{59}Co targets, evaporated on a Be or Al backing over a circular area 3 mm in diameter. The recoiling nuclei were collected on a set of concentric rings made of kapton or aluminum and placed 125 mm from the target perpendicular to the beam axis. The rings covered an angular range of 0° to 70° with respect to the beam and the widths of the individual rings corresponded to an angular step of 5° or 10°.

Results of the preliminary analysis of the data are shown in Figs. 1 through 5. In Figs. 1 and 2 the production cross sections for radioactive products and the recoil ranges are shown as a function of the laboratory bombarding energy. The solid curves represent the recoil range of the final nucleus if it were an evaporation product of a compound nucleus having the incident momentum of the projectile. The deviation of the observed recoil ranges from the solid curve marks the onset of nuclear reaction processes in which a significant fraction of the incident linear momentum is carried away by emission of forward-peaked, higher energy (compared to evaporation process) light particles and/or by transfer reactions. The first peak in the double-peaked excitation functions corresponds

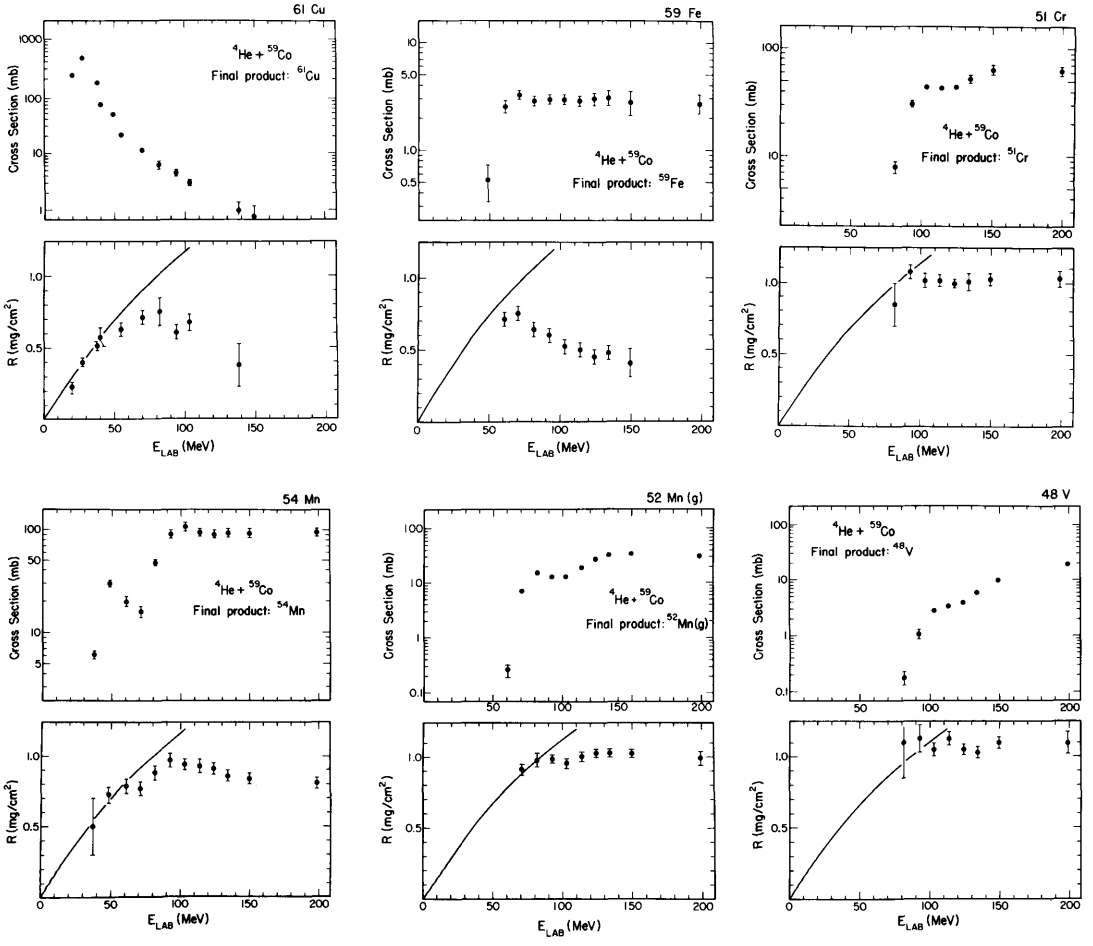

Figure 2. Cross sections (σ) and integral recoil ranges (R) plotted as a function of bombarding α-energy for the radioactive products of $^4He+^{59}Co$ reaction. The solid lines in the recoil ranges part of the figure are calculated assuming a full momentum transfer to the compound nucleus.

to the reaction process involving evaporation of at least one alpha-particle and the second to that involving only nucleon evaporation.

In Fig. 3, production cross sections, σ, for product nuclei of mass A_{RES} are plotted for four α-energies as a function of $\Delta A = A_{CN} - A_{RES}$ (A_{CN} is the mass of the compound nucleus). For each energy the ratio of the momentum, of the radioactive products along the beam axis $P_{||}$, to P_{CN}, the linear momentum a product would have if it were a residue of the initial compound nucleus, is plotted vs. ΔA. $P_{||}$ for a given A_{RES} was computed using the observed recoil range, the range-momentum relationship for ions of appropriate mass using the tables of Northcliffe and Schilling,[2] and the measured angular distribution of the recoil nuclei. Since the distributions of $P_{||}/P_{CN}$ observed

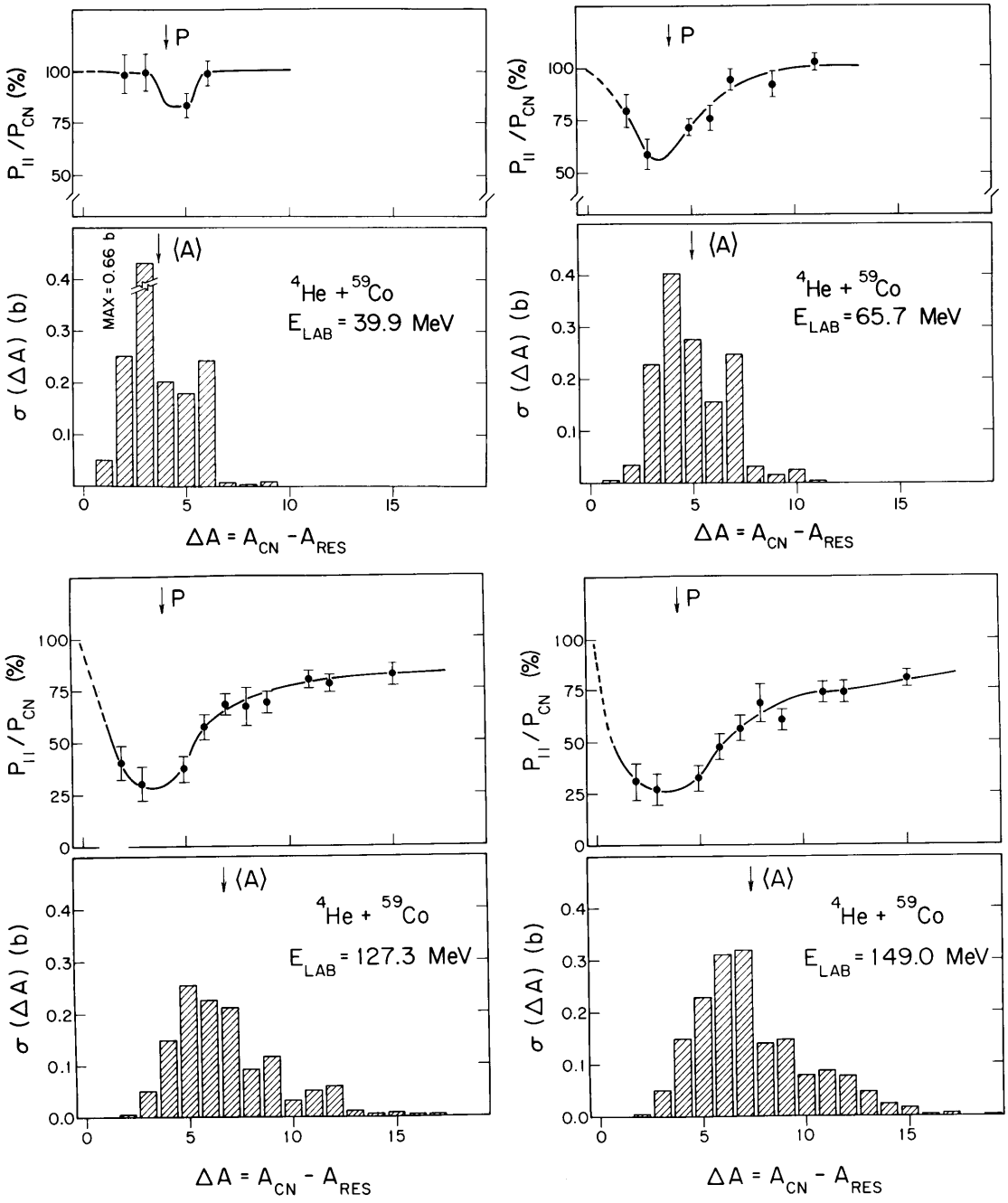

Figure 3. $P_{||}/P_{CN}$ and total cross sections as a function of $\Delta A = A_{CN} - A_{RES}$ for four bombarding energies. The arrow indicates the position of average mass removed from the compound nucleus at each energy. The lines are to guide the eye only.

for the radioactive nuclei are changing smoothly with ΔA, it is reasonable to assume that $P_{||}/P_{CN}$ of a nonradioactive nucleus is close to that observed for a radioactive nucleus of the same mass. Below an α-particle bombarding energy of about 50 MeV essentially all product nuclei have $P_{||}=P_{CN}$. At higher energies, one sees a decrease in $P_{||}/P_{CN}$ with ΔA, reaching a minimum with $\Delta A = 4$ or 5 and increasing with ΔA thereafter. At higher energies $P_{||}/P_{CN}$ appears to level off at ~70% for light product nuclei. The fact that the position of the minimum in $P_{||}/P_{CN}$ is independent of the bombarding energy and is localized near $\Delta A=4$ implies that final nuclei with mass close to, but lighter than, the target are produced via (α,α') followed by particle evaporation. Inelastically scattered α-particles carry away progressively lower fractions of the incident α-particle momentum with increasing excitation energy in the target; thus leading to increasing recoil momentum for lighter product nuclei. Clearly very light final nuclei are produced predominantly via evaporation from an initial highly-excited compound nucleus.

The average number of nucleons removed

$$\langle \Delta A \rangle = [\sum_i \sigma_i (A_{CN}-A_i)]/\sum_i \sigma_i,$$

and average value of transferred linear momentum

$$\langle P_{||}/P_{CN} \rangle = [\sum_i \sigma_i (P_{||}/P_{CN})]/\sum_i \sigma_i$$

are plotted as a function of the bombarding energy in Fig. 4. Below 50 MeV the slope of ΔA vs. E_α is about 1 nucleon per 10 MeV and falls to one nucleon per 37 MeV at higher energies. At 50 MeV $\langle P_{||}/P_{CN} \rangle$ drops below 100% and keeps falling monotonically beyond it. Both of these features are consistent with the idea that beyond around 50 MeV bombarding energy the

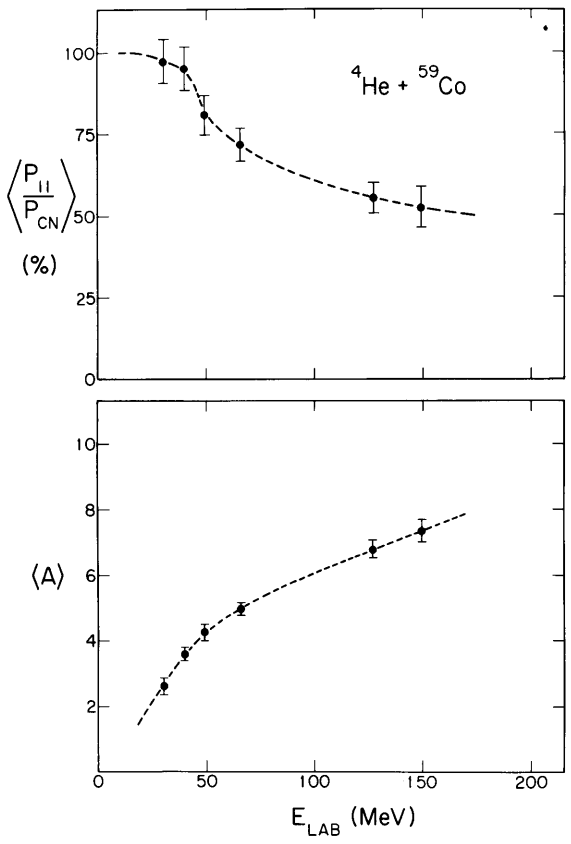

Figure 4. Energy dependence of the average value of transferred linear momentum $\langle P_{||}/P_{CN} \rangle$ and of average mass removed $\langle \Delta A \rangle$. The lines are to guide the eye only.

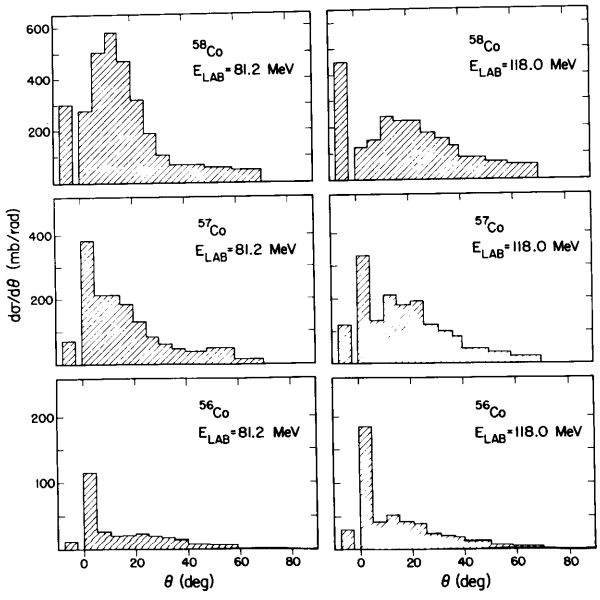

Figure 5. Angular distributions of radioactive Co isotopes at two bombarding energies. The area on the left of 0° represents the fraction of the activity left in the target.

non-compound nucleus formation processes start to dominate the reaction mechanism.

The angular distribution of the radioactive cobalt isotopes are shown in Fig. 5 at two energies. The narrow peaks in 0°-5° interval in each direction is consistent with the production of that nucleus from a forward recoiling compound nucleus through nucleon evaporation. Broad distributions at large angles must come from reaction processes such as (a,α') and other transfer reactions.

1) J. Jastrzebski, H.J. Karwowski, M. Sadler, and P.P. Singh, Phys. Rev. C 19, 724 (1979) and Phys. Rev. C 22, 1443 (1980).

2) L.C. Northcliffe and R.F. Schilling, Nuclear Data Tables, Vol. 7 (1970).